

Switching of optical vortices in nonlinear annular couplers

José R. Salgueiro

*Departamento de Física Aplicada, Universidade de Vigo,
Facultade de Ciencias de Ourense, E-32004 Ourense, Spain*

Yuri S. Kivshar

*Nonlinear Physics Center, Research School of Physical Sciences and Engineering,
Australian National University, ACT 0200 Canberra, Australia*

We suggest an annular waveguide coupler for switching the angular momentum of light. We study linear and nonlinear coupling of both power and momentum of an optical vortex beam launched into one of the ring cores, and demonstrate that the switching takes place well below the collapse threshold. The switching is more effective for the inner-ring excitation since it triggers more sharply and for the lower power enough to avoid the beam azimuthal instability.

PACS numbers:

Optical vortices are fundamental structures in the light fields associated with the points of vanishing intensity and phase singularities of optical beams [1]. Optical vortices are generated experimentally in different types of linear and nonlinear optical media [1, 2]. However, when a vortex beam propagates in a nonlinear medium, it becomes unstable due to the symmetry-breaking azimuthal instability [2], and it decays into several fundamental solitons [3]. Therefore, it is commonly accepted that any kind of an optical device operating with a transfer of the angular momentum of light and nonlinear switching of an optical vortex would be impossible due to this inherent instability and the subsequent vortex decay.

In a contrast with this common belief, in this Letter we suggest a novel type of a nonlinear waveguide coupler composed by two weakly coupled ring waveguides which not only preserve the angular momentum of the input light during the propagation, but also allow nonlinear switching for the beam power and angular momentum when it operates with ring-like optical vortex beams. Such two-ring annular waveguide couplers can be created, in particular, by a proper modulation of nondiffracting ring Bessel-like optical lattices [4] recently generated experimentally by the optical induction technique [5]. In this context, the ring solitons were studied in a multi-ring lattice for the case of a saturable nonlinearity [6].

The purpose of this Letter is twofold. First, we suggest a simple design of the nonlinear vortex coupler that is consistent with the conservation of the angular momentum of the vortex beam. Second, we study the angular momentum switching of the vortex in this coupler and compare it with the familiar switching observed for the beam power. We are interested how an input beam with a nonzero angular momentum can tunnel between the ring-like cores (either from the outer ring or from the inner ring) of the annular coupler, in both linear and nonlinear regimes. To the best of our knowledge, this problem has never been addressed before, but it seems very important for suggesting novel ways to manipulate, transform, and control the angular momentum of light. As a simple model, we consider a pair of two concentric step-index

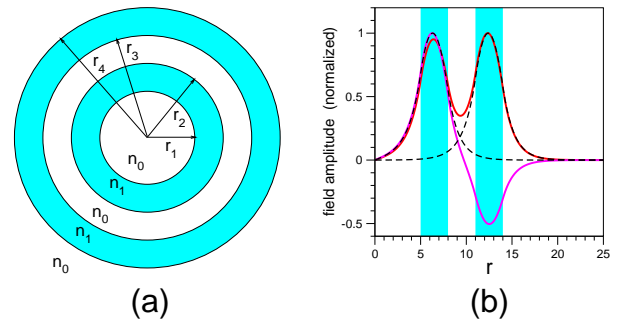


FIG. 1: (a) Sketch of an annular coupler. Values used for all simulations are $r_1 = 5$, $r_2 = 8$, $r_3 = 11$, $r_4 = 14$, $n_0 = 0$, $n_1 = 1$. (b) Continuous lines: radial profiles of the linear lowest-order vortex-type modes of the coupler with winding number $\ell = 1$ (symmetric, $\beta = 0.637$, and antisymmetric, $\beta = 0.594$). Dashed lines: radial profiles of the lowest-order vortex-type mode of each separate waveguide (inner: $\beta = 0.608$, outer: $\beta = 0.623$).

ring waveguides shown in Fig. 1(a). The two concentric cores and the substrate are made of two different materials with the refractive indices n_1 and n_0 , and both possessing a nonlinear Kerr response, so that the scalar optical field $\psi(r, \phi, z)$ propagating in the z -direction may be described by the normalized equation,

$$i \frac{\partial \psi}{\partial z} + \nabla_{\perp}^2 \psi + [V(r) + |\psi|^2] \psi = 0, \quad (1)$$

where ∇_{\perp}^2 is the Laplace operator, and $V(r)$ is the external potential of the double-ring coupler. Since we are interested in ring-shaped fields with nonzero angular momentum, the indices and dimensions of the coupler were chosen so that, for the linear regime, the coupler supports the usual symmetric and antisymmetric vortex-type modes [plotted in Fig. 1(b), solid]. Also, each of the waveguides, when considered separately, supports the lowest-order vortex-type radial mode [Fig. 1(b), dashed]. Those modes have the form,

$$\psi(r, \phi, z) = u(r) \exp(i\ell\phi) \exp(i\beta z), \quad (2)$$

where $u(r)$ is the radial profile of the corresponding mode, β is its propagation constant, and ℓ is the winding number that we fix as $\ell = 1$.

In our numerical simulations, we launch a vortex beam into one of the ring waveguides. We chose the initial radial shape of the field to be that of the single-waveguide mode [Fig. 1(b), dashed] in order to assure a good coupling to the ring-waveguide, although there would be no problem to take some other shape like Gaussian. The field is also initially scaled to establish the desired power and then propagates in a nonlinear regime. At each value of z , we characterize the vortex beam by calculating the beam power, $P = \int |\psi|^2 r dr d\phi$, and its angular momentum, $L_z = \text{Im}\{\int \psi^* \partial_\phi \psi r dr d\phi\}$, which are monitored for each waveguide. To do so, we consider a circular boundary just half way between both the cores and use all the points located in the inner part of this boundary to calculate the power and momentum for the inner core, and those in the external part to calculate those values for the external core. In Fig. 2, we show the intensity im-

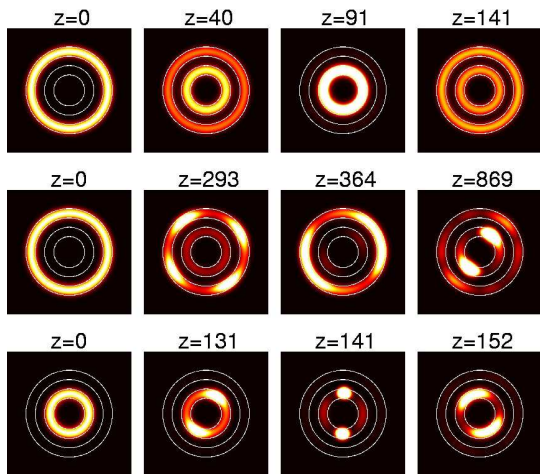


FIG. 2: Distribution of the light intensities in the coupler for different propagation distance z , for three different regimes. Top: external core excitation for the initial power $P = 5$. Center: external core excitation, at $P = 20$. Bottom: internal core excitation, at $P = 20$.

ages of the coupler for three different switching scenarios. Also, for both internal and external ring excitations, in Fig. 3 and Fig. 4 we plot the power and angular momentum for each waveguide together with their total values. Both magnitudes are in normalized units and on the same scale. In fact, according to the functional form of the input field (Eq. (2)), they are initially proportional,

$$L_z = \text{Im} \left\{ \int \psi^* \partial_\phi \psi = \ell \int u(r)^2 r dr \right\} = \ell P. \quad (3)$$

The top row in Fig. 2 shows the case of the external core excitation with a low power beam. A periodic coupling between both cores takes place and the beam remains stable. If power is increased (center row), the azimuthal

instability breaks the beam into a number of the fundamental solitons after some propagation distance. The larger the input power the shorter the propagation distance at which the breakup occurs. The resulting fundamental solitons present an oscillating width and rotate inside the ring due to the angular momentum, with an angular velocity that is larger as the the solitons width is smaller. If the input power is further increased, the fundamental solitons collapse as usual happens in the Kerr media. It is well known that for the nonlinear media with the focusing nonlinearity, solitons are unstable so that they either collapse or spread out. Due to the presence of the waveguides the spreading is stopped and so for low powers the beam remains stable.

Due to the proportionality relation between the momentum and power (see Eq. (3)), and the fact that we chose $\ell = 1$, the power and angular momentum have the same value meanwhile the beams remain unbroken (notice coincident thin and thick lines in Fig. 3 and Fig. 4). Nevertheless, it is notable that this parallel behavior diverges from the point where the beams breakup occurs due to the instabilities (notice a separation of the thin and thick lines), revealing differences in the momentum coupling. Besides, the total angular momentum is not longer conserved as is shown in the plots. Another in-

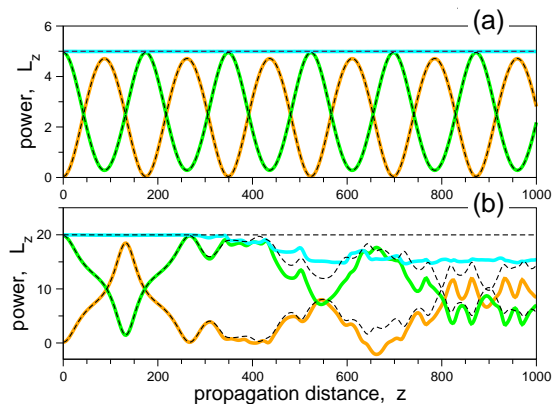


FIG. 3: Power (dashed lines) and angular momentum (continuous lines) in normalized units vs. propagation distance for outer-ring excitation. The individual values for each core are plotted, together with the total values. (a) simulation for $P=5$; (b) simulation for $P=20$.

teresting fact is the difference in suppression of coupling (switching) between internal and external ring excitation. When the external-ring core is excited, since it has a larger area, a higher power density is coupled into the inner core, and the beam breaks for a lower input power than the necessary to complete the switching. This is evident from Fig. 2(center row) where it is shown that after the beam breakage, coupling is still possible for a long enough propagation distance. To account for the switching property, we show the switching curves in Fig. 5, for power and angular momentum. They were built launching a single-ring field into one of the cores, simulating

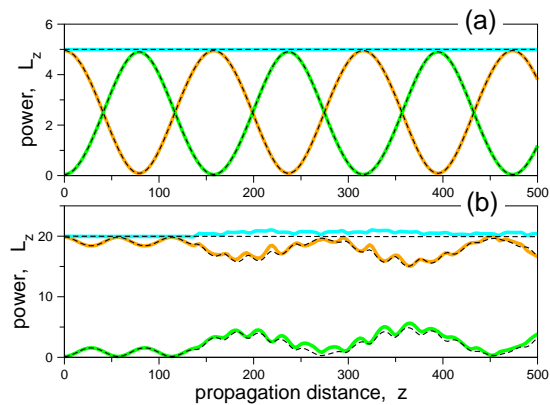


FIG. 4: Power (dashed lines) and angular momentum (continuous lines) vs. propagation distance for inner-ring excitation. The individual values for each core are plotted together with the total values. (a) simulation for $P=5$; (b) simulation for $P=20$.

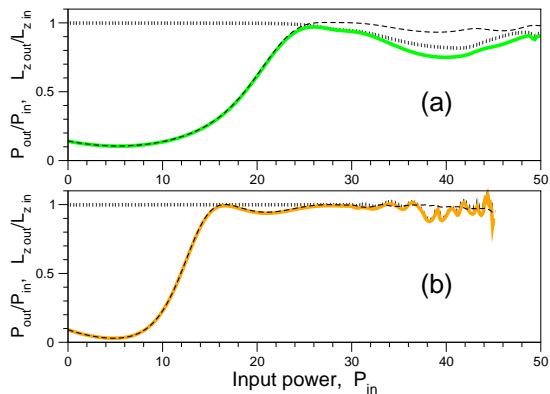


FIG. 5: Switching curves for the power (dark dashed lines) and angular momentum (light continuous lines) for (a) outer-waveguide excitation, and (b) inner-waveguide excitation. Also shown is the total angular momentum (dotted line).

the propagation for half a beating length and measuring the output power at the same core (the plot is the ratio between output and input power). The beating length is defined as the necessary distance to perform a complete coupling cycle (power transfer to the second core and

back to the first one), and was obtained by simulation in the linear regime. For the parameter values considered the half beating length resulted in $z=73.75$ and $z=73.85$ for internal and external ring excitation respectively.

Note that due to the asymmetry of the coupler (rings of different diameter), a complete transfer of power does not take place for the linear regime. That is why raising the power produces an initial increase of the coupled power and the switching curve presents an decreasing behavior at low powers. Also, for external core excitation, Fig. 5(a), the triggering is more steady and takes place at higher powers than for internal core excitation (b). This is due to the lower density of power in the external core because of its larger area.

The separation between the power and angular momentum curves denotes the point where the azimuthal instability breaks the beam before it propagates half a beating length. It happens clearly after switching took place in the case of internal excitation, but slightly before that point for external excitation. The curves reach an end-point when the power is so high that collapse takes place before the beam propagates for half a beating length.

In conclusion, we have suggested a novel design of a nonlinear optical coupler for switching the angular momentum of light. We have studied numerically the operation of such a coupler and demonstrated that a low-power optical vortex launched into one of the ring waveguides transfers periodically between both rings with a perfect periodic change of both beam power and its angular momentum. From the study of the nonlinear regime (larger power) of the coupler we draw the conclusion that the internal excitation is more effective since the slope of the switching curve is larger and switching is triggered well before the beam breaks up due to the azimuthal instability. For outer-ring excitation, however, it is still possible to perform the switching for powers low enough to avoid the beam collapse.

JRS acknowledges the Ramón y Cajal contract from the Ministerio de Educación y Ciencia of Spain and a support from Xunta de Galicia (project PGIDIG06PXIB239155PR). YK acknowledges a support from the Australian Research Council.

[1] See, e.g. M.S. Soskin and M.V. Vasnnetsov, in *Progress in Optics* Vol. **42**, Ed. E. Wolf, (North-Holland, Amsterdam, 2001) p. 219; and references therein.
 [2] A.S. Desyatnikov, Yu.S. Kivshar, and L. Torner, in *Progress in Optics* Vol. **47**, Ed. E. Wolf, (North-Holland, Amsterdam, 2005) pp. 291–391.
 [3] See, e.g., Yu.S. Kivshar and G. Agrawal, *Optical Solitons: From Fibers to Photonic Crystals* (Academic Press, San

Diego, 2003), Sec. 6.5.
 [4] Y.V. Kartashov, V.A. Vysloukh, and L. Torner, *Phys. Rev. Lett.* **93**, 093904 (2004).
 [5] X. Wang, Z. Chen, and P.G. Kevrekidis, *Phys. Rev. Lett.* **96**, 083904 (2006).
 [6] Q.E. Hoq, P.G. Kevrekidis, D.J. Frantzeskakis, and B.A. Malomed, *Phys. Lett. A* **341**, 145 (2006).